HHS Public Access

Author manuscript

J Photochem Photobiol B. Author manuscript; available in PMC 2018 February 01.

Published in final edited form as:

J Photochem Photobiol B. 2017 February ; 167: 111–116. doi:10.1016/j.jphotobiol.2016.12.018.

A PSMA-Targeted Theranostic Agent for Photodynamic Therapy

Ying Chen[*], **Samit Chatterjee**, **Ala Lisok**, **Il Minn**, **Mrudula Pullambhatla**, **Bryan Wharram**, **Yuchuan Wang**, **Jiefu Jin**, **Zaver M. Bhujwalla**, **Sridhar Nimmagadda**, **Ronnie C. Mease**, and **Martin G. Pomper**[*]

Russell H. Morgan Department of Radiology and Radiological Science Johns Hopkins Medical Institutions, Baltimore, MD 21287

Abstract

Prostate-specific membrane antigen (PSMA) is over-expressed in the epithelium of prostate cancer and in the neovasculature of many non-prostate solid tumors. PSMA has been increasingly used as a target for cancer imaging and therapy. Here we describe a low-molecular-weight theranostic photosensitizer, **YC-9**, for PSMA-targeted optical imaging and photodynamic therapy (PDT). **YC-9** was synthesized by conjugating IRDye700DX *N*-hydroxysuccinimide (NHS) ester with a PSMA targeting Lys-Glu urea through a lysine-suberate linker in suitable yield. Optical imaging *in vivo* demonstrated PSMA-specific tumor uptake of **YC-9** with rapid clearance from non-target tissues. PSMA-specific cell kill was demonstrated with **YC-9** *in vitro* through PDT in $PSMA^+$ PC3-PIP and $PSMA^-$ PC3-flu cells. *In vivo* PDT in mice bearing $PSMA^+$ PC3-PIP tumors at 4 h post-injection of **YC-9** (A total of four PDT sessions were performed, 48 h apart) resulted in significant tumor growth delay, while tumors in control groups continued to grow. PDT with **YC-9** significantly increased the median survival of the $PSMA^+$ PC3-PIP tumor mice (56.5 days) compared to other control groups [23.5-30.0 days, including untreated, light alone, **YC-9** alone (without light) and non-targeted IRDye700DX PDT treatment groups], without noticeable toxicity at the doses used. This study proves in principle that **YC-9** is a promising therapeutic agent for targeted PDT of PSMA-expressing tissues, such as prostate tumors and may also be useful against non-prostate tumors by virtue of neovascular PSMA expression.

Keywords

prostate-specific membrane antigen; prostate cancer; PDT; optical imaging; molecular imaging

Corresponding Authors: Martin G. Pomper, M.D., Ph.D. Johns Hopkins Medical School 1550 Orleans Street, 492 CRB II Baltimore, MD 21287: mpomper@jhmi.edu, Ying Chen, Ph.D. Johns Hopkins Medical School 1550 Orleans Street, 470 CRB II Baltimore, MD 21287: ychen95@jhmi.edu.

Competing Interests: The authors have declared that no competing interest exists.

Introduction

New treatments for cancer are becoming less invasive and more targeted. Desirable targets for cancer treatment include those expressed at high levels within a variety of tumor types or within tumor neovasculature. PSMA, also known as glutamate carboxypeptidase II (GCPII), *N*-acetylated-α-linked acidic dipeptidase (NAALADase) or folate hydrolase 1 (FOLH1), is a type II integral membrane protein expressed on the surface of prostate tumors, particularly in castration-resistant, advanced and metastatic disease [1, 2]. PSMA is also expressed in the neovascular endothelium of most solid tumors such as lung, colon, pancreas, renal cell and melanoma, but not in normal vasculature [3, 4]. It represents an excellent target for imaging and targeted therapy of cancer.

Photodynamic therapy (PDT) is a minimally invasive cancer treatment that is FDA-approved for locally advanced esophageal and lung cancers and is under investigation for many other light-accessible cancers, such as prostate, skin, head and neck, bladder, renal cell, cervix, and pancreas [5]. The principle of PDT involves intravenous or topical administration of a chemical (photosensitizer) that is activated by light. This is followed by local irradiation using light with an appropriate wavelength, often through fiber optics. Energy is transferred from the photosensitizer to molecular oxygen to generate reactive oxygen species (ROS) that attack and destroy nearby cells. In addition to killing cancer cells directly, PDT can shrink or eradicate tumors by destroying the endothelium of tumor neovasculature [5]. PDT has several advantages over conventional therapies such as surgery, radiation therapy and chemotherapy because it is minimally invasive and can be used repeatedly without limitation of the total dose or treatment resistance [6]. PDT provides a level of tumor selectivity through control of what tissues are irradiated after administration of the photosensitizer. A second level of selectivity is provided by passive accumulation of photosensitizers within tumors by virtue of abnormal vasculature and lymphatics unique to tumors. Unfortunately, the non-specific distribution of the systemic photosensitizers often results in suboptimal treatment outcomes and prolonged photosensitivity in healthy tissues [7]. A major goal of cancer PDT is to improve the tumor-specific delivery of photosensitizers through active targeting to enhance efficacy while reducing the administered dose of photosensitizer to minimize side effects [8-16]. Since PSMA is over-expressed on prostate cancer and the neovasculature of numerous solid tumors that can be assessed with light either directly or endoscopically, it is a suitable target for PDT.

Recently, Watanabe *et al.* reported effective PSMA-targeted photoimmunotherapy by targeting with both full antibodies and antibody fragments [17]. When compared to antibody or antibody fragments, low molecular weight (LMW) agents may have better pharmacokinetics and faster clearance due to their small size. Previously, Liu *et al.* reported that pyropheophorbide-a conjugated peptidomimetic LMW PSMA inhibitors for targeted PDT demonstrated selective targeting and efficacy for PDT *in vitro*; however, no data have been reported on *in vivo* PDT [18-20]. We and others have synthesized a variety of LMW PSMA-targeted radiotracers and optical agents to enable imaging of prostate cancer [21]. In particular, most of those agents utilized the PSMA binding moiety Lys-Glu urea [22-25]. Several of those agents are under clinical investigation [26-32]. Recently we reported the synthesis and preliminary evaluation of a PSMA-targeted Lys-Glu urea based theranostic

agent **YC-9** for prostate cancer optical imaging and PDT [33]. Here we report in more detail the synthesis of this agent and its *in vitro* and *in vivo* evaluation for PDT. While this paper was in preparation, Wang *et al.* published PSMA-targeted PDT agents utilizing the PSMA binding Glu-Glu urea moiety [34].

Materials and Methods

General

Reagents and solvents were purchased from either Sigma-Aldrich (Milwaukee, WI) or Fisher Scientific (Pittsburgh, PA). The trifluoroacetate salt of 2-(3-{5-[7-(5-amino-1-carboxy-pentylcarbamoyl)-heptanoylamino]-1-carboxy-pentyl}-ureido)-pentanedioic acid **1** [22] (Figure 1) was prepared according to our published procedure. IRDye700DX NHS ester was purchased from LI-COR Biosciences (Lincoln, NE). ESI mass spectra were obtained on a Bruker Esquire 3000 plus system. Purification by high performance liquid chromatography (HPLC) was performed on a Varian Prostar System (Palo Alto, CA).

Synthesis of YC-9

N,N-Diisopropylethylamine (0.005 mL, 28.8 μmol) was added to a solution of **1** (0.5 mg, 0.70 μmol) in DMSO (0.1 mL), followed by IRDye700DX NHS ester (0.5 mg, 0.26 μmol). After stirring for 1 h at room temperature, the reaction mixture was purified by HPLC (column, Alltech Econosphere C18 5μ, 150 × 4.6 mm; retention time, 22 min; mobile phase, A = 10 mM triethylammonium acetate (pH 7.0), B = MeOH; gradient, 0 min = 5% B, 5 min = 5% B, 45 min = 100% B; flow rate, 1 mL/min) to afford 0.4 mg (67%) of **YC-9**. ESI-Mass calcd for $C_{96}H_{138}N_{16}O_{35}S_6Si_3$ $[M-2H]^{2-}$, 1175.9, found 1175.3.

NAALADase assay

The PSMA inhibitory activity of **YC-9** was determined using a fluorescence-based assay according to a previously reported procedure [36]. Briefly, lysates of $PSMA^+$ LNCaP cell extracts (25 μL) were incubated with **YC-9** (12.5 μL) in the presence of 4 μM *N*-acetylaspartylglutamate (NAAG) (12.5 μL) for 120 min at 37°C. The amount of the released glutamate by NAAG hydrolysis was measured by incubating with a working solution (50 μL) of the Amplex Red Glutamic Acid Kit (Molecular Probes Inc., Eugene, OR, USA) for 60 min. Fluorescence was measured with a VICTOR3V multilabel plate reader (Perkin Elmer Inc., Waltham, MA) with excitation at 490 nm and emission at 642 nm. Inhibition curves were determined using semi-log plots and IC_{50} values were determined at the concentration at which enzyme activity was inhibited by 50%. Assays were performed in triplicate. Enzyme inhibitory constants (K_i values) were generated using the Cheng-Prusoff conversion [35]. Data analysis was performed using GraphPad Prism version 4.00 for Windows.

Cell culture

Both PSMA-expressing (PC3-PIP) and non-expressing (PC3-flu) prostate cancer cell lines were grown in RPMI 1640 medium (Invitrogen, Carlsbad, California) containing 10% fetal bovine serum (FBS) (Invitrogen) and 1% Pen-Strep (Biofluids, Camarillo, California). Cell

cultures were maintained under 5% carbon dioxide (CO_2), at 37.0°C in a humidified incubator.

In vitro PDT

The photosensitizer concentration used in *in vitro* PDT studies was based on the **YC-9** concentration that saturates *in vitro* uptake measured by flow cytometry. $PSMA^+$ PC3-PIP and $PSMA^-$ PC3-flu cells (1×10^5) were plated on 24-well plate on day 1. On day 2 cells were incubated 1) with no added compound, 2) with IRDye700DX (100 nM), and 3) with **YC-9** (100 nM) for 1 h at 37°C. After washing twice with media, cells were either irradiated with an LED light source (L690-66-60, Marubeni America Co., Santa Clara, CA, wavelength: 690 ± 20 nm; total fluence: 2 J/cm^2) or were not irradiated. Cell viability was measured by XTT assay (American Type Culture Collection, Manassas, VA) 24 h post-irradiation. Statistical significance was calculated using the Student's *t*-test.

In vivo optical imaging and *ex vivo* biodistribution

Animal studies were carried out in compliance with the regulations of the Johns Hopkins Animal Care and Use Committee. Six- to eight-week-old male, non-obese diabetic (NOD)/severe-combined immunodeficient (SCID) mice were purchased from the Johns Hopkins Immunocompromised Animal Core. For *in vivo* imaging, mice were implanted subcutaneously with $PSMA^+$ PC3-PIP and $PSMA^-$ PC3-flu cells (2×10^6 in 100 μL PBS) at the forward right and left flanks, respectively. Mice were imaged and used in *ex vivo* biodistribution studies when the xenografts reached approximately 5 to 7 mm in diameter. Following intravenous (IV) injection of 10 nmol **YC-9** in PBS, mice were imaged at 6 h and 24 h post-injection (pi) using a dedicated small animal optical imaging instrument, the Pearl Impulse™ Imager (LI-COR Biosciences, Lincoln, NE). All images were acquired with the 700 nm channel and were scaled to the same maximum values. The imaging bed temperature was maintained at 37°C. Animals received inhalational anesthesia (isoflurane) through a nose cone attached to the imaging bed. At the end of image acquisition, animals were sacrificed by cervical dislocation for imaging *ex vivo*. Organs and tumors imaged included liver, spleen, stomach, small intestine, kidneys, muscle, $PSMA^+$ PC3-PIP and $PSMA^-$ PC3-flu tumors.

In vivo PDT

Six- to eight-week-old male NOD-SCID mice (obtained from The Johns Hopkins Immune Compromised Animal Core) were used for *in vivo* PDT. Mice were implanted subcutaneously with $PSMA^+$ PC3-PIP cells (2×10^6 in 100 μL PBS) on the right hind flank. When the xenograft volumes reached approximately 50 mm^3, hair removal cream (Reckitt Benckiser Inc, Parsippany, NJ) was applied around the tumor to remove the fur. Mice were then randomly distributed to five groups (six mice/group). The treatments for each group are shown in Table 1.

A LED light source (L690-66-60; Marubeni America Co., Santa Clara, CA; wavelength: 690 ± 20 nm, total fluence: 100 J/cm^2) was used for light treatment. A total of four PDT sessions were performed, 48 h apart. The effect of *in vivo* PDT was studied by long-term tumor response and by histologic evaluation of tumor sections at 24 h after the first and fourth PDT

treatment. Body weights of mice were also recorded to monitor their overall health during the study. The tumor growth of the mice was measured with calipers every 2-3 days until euthanasia. Tumor volumes were calculated by the modified ellipsoidal formula: (length × width^2)/2. The tumor growth curves and the Kaplan-Meier analyses were plotted using Graphpad Prism software. Statistical significance was calculated using one-way ANOVA. When the *P*-value was < 0.05, the difference between the compared groups was considered to be statistically significant.

Histology

PSMA$^+$ PC3-PIP tumors from PDT treated or untreated control mice were harvested at 24 h after the first and fourth PDT treatment and fixed in 10% buffered formalin. Tissues were subsequently embedded in paraffin and sectioned at 4 μm thickness. Tissue sections were stained with hematoxylin and eosin (H&E) to visualize gross morphology. A standard immunohistochemical protocol was followed to stain the tissue sections with either anti-Ki-67 antibody (1:500 dilution, polyclonal, Novus, Littleton, CO), anti-cleaved caspase-3 antibody(1:800 dilution, clone 5A1E, Cell Signaling, Danvers, MA) or anti-PSMA antibody (1:50 dilution,Clone 3E6, Dako, Carpinteria, CA). Briefly, slides were deparaffinized by xylene wash andalcohol gradients, treated with antigen retrieval buffer, blocked with 3% H_2O_2 for 10 min,blocked with 10% FBS for 30 min and then incubated with the primary antibody overnight in ahumidified chamber at room temperature. Slides were subsequently washed and then incubated with secondary anti rabbit polymer HRP (for Ki-67 and cleaved caspase-3) or anti-mousepolymer HRP (for PSMA) (used undiluted, Dako) for 15 min at room temperature. DAB staining was done according to the manufacturer's protocol (Dako). Sections were counterstained with hematoxylin solution (Sigma, prepared as DI H_2O: stain = 6:1) followed by dehydration with alcohol gradients and xylene washes and finally mounted with a cover slip. Quantification of immunohistochemical staining was performed by using the ImageJ software.

Results and Discussion

PDT has received increased attention in recent years due to the availability of new efficient photosensitizers and laser sources. Classical, non-targeted photosensitizers lack sufficient tumor selectivity and result in suboptimal treatment outcomes and undesirable side effects [7]. Targeted PDT may improve the treatment efficacy and reduce systemic toxicity. We previously reported **YC-27**, the first LMW PSMA-targeted fluorescent imaging agent capable of imaging prostate cancer *in vivo* [22]. Recently, we extended that work by synthesizing and testing a series of PSMA-targeted near-infrared (NIR) fluorescent imaging agents with different linkers and fluorophores [25]. Building upon those results we again turned to the urea scaffold to generate photosensitizer **YC-9** for PSMA-targeted PDT.

YC-9 consists of three functional parts: 1) photosensitizer IRDye700DX, 2) PSMA-targeting moiety Lys-Glu urea, and 3) a lysine-suberate linker that tethers the PSMA binding urea to the bulky photosensitizer. **YC-9** was synthesized in suitable yield (67%) from commercially available IRDye700DX NHS ester and PSMA-binding urea **1** under mild conditions (Figure 1). I*n vitro* PSMA inhibitory activity of **YC-9** using a fluorescence-based

NAALADase assay [36] demonstrated a K_i of 0.2 nM with 95% confidence intervals ranging from 0.15 nM to 0.25 nM. **YC-9** exhibited 5-10 fold higher affinity than the known potent PSMA inhibitor ZJ-43 (K_i 1.8 nM), under the same experimental conditions.

We initially tested the PDT therapeutic effect of **YC-9** *in vitro* and observed **YC-9** induced PSMA-specific PDT. In particular, we observed a 99.8% cell kill in $PSMA^+$ PC3-PIP cells treated with **YC-9** followed by light irradiation, but not in control $PSMA^-$ PC3-flu cells (Figure 2). Other controls, including treatment with light alone, **YC-9** alone (without light) and non-targeted IRDye700DX dye (with or without light) did not show appreciable cell kill. These results demonstrate that **YC-9** possesses PSMA-specific phototoxicity, and negligible *in vitro* cytotoxicity in the absence of light irradiation.

YC-9 emits NIR fluorescence allowing optical imaging *in vivo*, in addition to being a photosensitizer to generate singlet oxygen for PDT. We hypothesize that optical imaging can be utilized to measure **YC-9** tumor distribution kinetics *in vivo* and optimization of PDT delivery. Therefore, we used NIR imaging to study the pharmacokinetics of **YC-9** in mice. Figure 3 (top panel) shows typical whole body and excised organ images of mice with $PSMA^+$ PC3-PIP and $PSMA^-$ PC3-flu tumors at 6 and 24 h post-injection of 10 nmol of **YC-9**. We observed high uptake of **YC-9** in the $PSMA^+$ PC3-PIP tumor and very low uptake in the $PSMA^-$ PC3-flu tumor. Rapid clearance from off-target sites and specific and high retention in $PSMA^+$ PC3-PIP tumors was observed, resulting in significant target-to-non-target contrast at 24 h. These observations were further confirmed by similar results observed with NIR imaging of excised tissues at 24 h. The kidney uptake was partially due to the route of excretion as well as high expression of PSMA within proximal renal tubules [37]. We anticipate that toxicity associated with such highly specific agents is further reduced by: i) the fast clearance rate observed from non-target tissues; ii) low concentration of PDT agents used; iii) tissue or organ specific and focused irradiation required for PDT. Although we did not observe any reduction in weight of mice undergoing therapy, an indicator of cumulative toxicity, detailed investigation into toxicity of these agents is necessary prior to clinical translation.

To demonstrate further PSMA-binding specificity of **YC-9**, we co-administered a 100-fold excess of 2-{3-[1-carboxy-5-(4-iodobenzoylamino)-pentyl]-ureido}-pentanedioic acid (DCIBzL, a potent PSMA inhibitor, 1 μmol)[36] with **YC-9**. As shown in Figure 3 (bottom panel), the light emission from the $PSMA^+$ PC3-PIP tumor was markedly reduced with concurrent DCIBzL administration, indicating PSMA-specific binding of **YC-9**.

In vivo PDT treatment demonstrated that **YC-9** PDT (**YC-9** + light) resulted in tumor growth delay. Tumor shrinkage was observed in all of the $PSMA^+$ PC3-PIP tumors as early as two days after the start of treatment, while tumors in control groups continued to grow (Figure 4A). Controls included untreated, light alone, **YC-9** alone (without light), non-targeted IRDye700DX + light treatment groups. **YC-9** PDT significantly increased the median survival of the $PSMA^+$ PC3-PIP tumor mice (Figure 4B). We observed that median survival time (56.5 days) nearly doubled in the **YC-9** PDT group compared to controls (23.5-30.0 days, $P = 0.0003$) (Figure 4C), based on a pseudo-survival Kaplan-Meier plot generated for the time to reach a ten-fold in size over the initial tumor volume. **YC-9** PDT

was also well tolerated as indicated by lack of change in body weight. These results collectively demonstrate that **YC-9** PDT causes tumor regression and delay in tumor growth without noticeable toxicity at the doses used, which are similar with the *in vivo* treatment results published by Wang *et al.* [34]

To investigate therapy-induced changes in the tumors, histological and immunohistochemical assessments were performed on $PSMA^+$ PC3-PIP tumors harvested 24 h after the first and fourth **YC-9** PDT treatments, and also on untreated control $PSMA^+$ PC3-PIP tumors. Untreated control tumors showed very high levels of PSMA expression, which was reduced by 55% after one PDT treatment and further decreased by the fourth PDT session (Figure 5A). Untreated control tumor sections exhibited intense Ki-67 staining that can be attributed to the higher cellular proliferation compared to PDT treated tumor (Figure 5B). Treated tumor sections also exhibited significant cleaved caspase-3 staining (Figure 5C), suggesting the occurrence of apoptosis and subsequent cell death following therapy. H&E staining of treated tumor sections showed greater tumor cell death and increased overall cellular damage compared to controls (Figure 5D). The effect of PDT on cell proliferation and cell death was more conspicuous after the fourth dose than after the first dose (Figure 5B-D). Collectively, these data of molecular characterization substantiate the observed changes in tumor growth.

In conclusion, this study proves in principle that **YC-9** is a promising therapeutic agent for targeted PDT of PSMA-expressing tissues, such as prostate tumors and may be useful against non-prostate tumors by virtue of neovascular PSMA expression. Our results along with those of Wang et al [34] lend support to the efficacy of PSMA-targeted PDT using LMW agents.

Acknowledgments

We thank CA134675 and CA103175 for financial support, and Dr. Hisataka Kobayashi for helpful discussions.

References

1. Huang X, Bennett M, Thorpe PE. Anti-tumor effects and lack of side effects in mice of animmunotoxin directed against human and mouse prostate-specific membrane antigen. Prostate. 2004; 61:1–11. [PubMed: 15287089]
2. Schuelke N, Varlamova OA, Donovan GP, Ma D, Gardner JP, Morrissey DM, Arrigale RR, Zhan C, Chodera AJ, Surowitz KG, Maddon PJ, Heston WDW, Olson WC. The homodimer of prostate-specific membrane antigen is a functional target for cancer therapy. Proc Natl Acad Sci. 2003; 100:12590–12595. [PubMed: 14583590]
3. Liu H, Moy P, Kim S, Xia Y, Rajasekaran A, Navarro V, Knudsen B, Bander NH. Monoclonal antibodies to the extracellular domain of prostate-specific membrane antigen also react with tumor vascular endothelium. Cancer research. 1997; 57:3629–3634. [PubMed: 9288760]
4. Chang SS, Reuter VE, Heston WD, Bander NH, Grauer LS, Gaudin PB. Five different anti-prostate-specific membrane antigen (PSMA) antibodies confirm PSMA expression in tumor-associated neovasculature. Cancer research. 1999; 59:3192–3198. [PubMed: 10397265]
5. Triesscheijn M, Baas P, Schellens JHM, Stewart FA. Photodynamic therapy in oncology. Oncologist. 2006; 11:1034–1044. [PubMed: 17030646]
6. Wilson BC, Patterson MS. The physics, biophysics and technology of photodynamic therapy. Phys Med Biol. 2008; 53:R61–109. [PubMed: 18401068]

7. Celli JP, Spring BQ, Rizvi I, Evans CL, Samkoe KS, Verma S, Pogue BW, Hasan T. Imaging and Photodynamic Therapy: Mechanisms, Monitoring, and Optimization. Chemical Reviews. 2010; 110:2795–2838. [PubMed: 20353192]
8. Maziere JC, Morliere P, Santus R. The role of the low density lipoprotein receptor pathway in the delivery of lipophilic photosensitizers in the photodynamic therapy of tumours. J Photochem Photobiol B. 1991; 8:351–360. [PubMed: 1904487]
9. Lutsenko SV, Feldman NB, Finakova GV, Posypanova GA, Severin SE, Skryabin KG, Kirpichnikov MP, Lukyanets EA, Vorozhtsov GN. Targeting phthalocyanines to tumor cells using epidermal growth factor conjugates. Tumour Biol. 1999; 20:218–224. [PubMed: 10393532]
10. Swamy N, James DA, Mohr SC, Hanson RN, Ray R. An estradiol-porphyrin conjugate selectively localizes into estrogen receptor-positive breast cancer cells. Bioorg Med Chem. 2002; 10:3237–3243. [PubMed: 12150869]
11. Khan EH, Ali H, Tian H, Rousseau J, Tessier G, Shafiullah, van Lier JE. Synthesis and biologicalactivities of phthalocyanine-estradiol conjugates. Bioorg Med Chem Lett. 2003; 13:1287–1290. [PubMed: 12657265]
12. Stevens PJ, Sekido M, Lee RJ. Synthesis and evaluation of a hematoporphyrin derivative in a folate receptor-targeted solid-lipid nanoparticle formulation. Anticancer Res. 2004; 24:161–165. [PubMed: 15015592]
13. Savellano MD, Pogue BW, Hoopes PJ, Vitetta ES, Paulsen KD. Multiepitope HER2 targeting enhances photoimmunotherapy of HER2-overexpressing cancer cells with pyropheophorbide-a immunoconjugates. Cancer Res. 2005; 65:6371–6379. [PubMed: 16024640]
14. Kuimova MK, Bhatti M, Deonarain M, Yahioglu G, Levitt JA, Stamati I, Suhling K, Phillips D. Fluorescence characterisation of multiply-loaded anti-HER2 single chain Fv-photosensitizer conjugates suitable for photodynamic therapy. Photochem Photobiol Sci. 2007; 6:933–939. [PubMed: 17721591]
15. Mitsunaga M, Ogawa M, Kosaka N, Rosenblum LT, Choyke PL, Kobayashi H. Cancer cell-selective in vivo near infrared photoimmunotherapy targeting specific membrane molecules. Nat Med. 2011; 17:1685–1691. [PubMed: 22057348]
16. Nakajima T, Mitsunaga M, Bander NH, Heston WD, Choyke PL, Kobayashi H. Targeted, activatable, in vivo fluorescence imaging of prostate-specific membrane antigen (PSMA) positive tumors using the quenched humanized J591 antibody-indocyanine green (ICG) conjugate. Bioconjug Chem. 2011; 22:1700–1705. [PubMed: 21740058]
17. Watanabe R, Hanaoka H, Sato K, Nagaya T, Harada T, Mitsunaga M, Kim I, Paik CH, Wu AM, Choyke PL, Kobayashi H. Photoimmunotherapy targeting prostate-specific membrane antigen: are antibody fragments as effective as antibodies? Journal of nuclear medicine : official publication, Society of Nuclear Medicine. 2015; 56:140–144.
18. Liu T, Wu LY, Choi JK, Berkman CE. In vitro targeted photodynamic therapy with a pyropheophorbide-a conjugated inhibitor of prostate-specific membrane antigen. Prostate. 2009; 69:585–594. [PubMed: 19142895]
19. Liu T, Wu LY, Choi JK, Berkman CE. Targeted photodynamic therapy for prostate cancer: inducing apoptosis via activation of the caspase-8/-3 cascade pathway. Int J Oncol. 2010; 36:777–784. [PubMed: 20198319]
20. Liu T, Wu LY, Berkman CE. Prostate-specific membrane antigen-targeted photodynamic therapy induces rapid cytoskeletal disruption. Cancer Lett. 2010; 296:106–112. [PubMed: 20452720]
21. Kiess AP, Banerjee SR, Mease RC, Rowe SP, Rao A, Foss CA, Chen Y, Yang X, Cho SY, Nimmagadda S, Pomper MG. Prostate-specific membrane antigen as a target for cancer imaging and therapy. The quarterly journal of nuclear medicine and molecular imaging : official publication of the Italian Association of Nuclear Medicine. 2015; 59:241–268.
22. Chen Y, Dhara S, Banerjee SR, Byun Y, Pullambhatla M, Mease RC, Pomper MG. A low molecular weight PSMA-based fluorescent imaging agent for cancer. Biochemical and Biophysical Research Communications. 2009; 390:624–629. [PubMed: 19818734]
23. Maresca KP, Hillier SM, Femia FJ, Keith D, Barone C, Joyal JL, Zimmerman CN, Kozikowski AP, Barrett JA, Eckelman WC, Babich JW. A series of halogenated heterodimeric inhibitors of prostate

specific membrane antigen (PSMA) as radiolabeled probes for targeting prostate cancer. J Med Chem. 2009; 52:347–357. [PubMed: 19111054]

24. Chen Y, Pullambhatla M, Foss CA, Byun Y, Nimmagadda S, Senthamizhchelvan S, Sgouros G, Mease RC, Pomper MG. 2-(3-{1-Carboxy-5-[(6-[18F]Fluoro-Pyridine-3-Carbonyl)-Amino]-Pentyl}-Urei do)-Pentanedioic Acid, [18F]DCFPyL, a PSMA-Based PET Imaging Agent for Prostate Cancer. Clin Cancer Res. 2011; 17:7645–7653. [PubMed: 22042970]
25. Chen Y, Pullambhatla M, Banerjee SR, Byun Y, Stathis M, Rojas C, Slusher BS, Mease RC, Pomper MG. Synthesis and Biological Evaluation of Low Molecular Weight Fluorescent Imaging Agents for the Prostate-Specific Membrane Antigen. Bioconjugate chemistry. 2012; 23:2377–2385. [PubMed: 23157641]
26. Cho SY, Gage KL, Mease RC, Senthamizhchelvan S, Holt DP, Kwanisai-Jeffrey A, Endres CJ, Dannals RF, Sgouros G, Lodge MA, Eisenberger MA, Rodriguez R, Carducci MA, Rojas C, Slusher BS, Kozikowski AP, Pomper MG. Biodistribution, Tumor Detection and Radiation Dosimetry of N-[N-[(S)-1,3-Dicarboxypropyl]carbamoyl]-4-18F-fluorobenzyl-L-cysteine (18F-DCFBC), a Low Molecular Weight Inhibitor of PSMA, in Patients with Metastatic Prostate Cancer. J Nucl Med. 2012; 53:1883–1891. [PubMed: 23203246]
27. Barrett JS, LaFrance N, Coleman RE, Goldsmith SJ, Stubbs JB, Petry NA, Vallabhajosula S, Maresca KP, Femia FJ, Babich JW. Targeting metastatic prostate cancer (PCA) in patients wtih 123I-MIP1072 and 123I-MIP1095. Annual Meeting of the Society of Nuclear Medicine. 2009:36P.
28. Babich J, Coleman RE, Van Heertum R, Vallabahajosula S, Goldsmith S, Osborne J, Slawin K, Joyal J. Small molecule inhibitors of prostate specific membrane antigen (PSMA) for SPECT: Summary of phase I studies in patients with prostate cancer (PCa). Annual Meeting of the Society of Nuclear Medicine. 2012:179P.
29. Afshar-Oromieh A, Haberkorn U, Eder M, Eisenhut M, Zechmann CM. [68Ga]Gallium-labelled PSMA ligand as superior PET tracer for the diagnosis of prostate cancer: comparison with 18F-FECH. Eur J Nucl Med Mol Imaging. 2012; 39:1085–1086. [PubMed: 22310854]
30. Szabo Z, Mena E, Rowe SP, Plyku D, Nidal R, Eisenberger MA, Antonarakis ES, Fan H, Dannals RF, Chen Y, Mease RC, Vranesic M, Bhatnagar A, Sgouros G, Cho SY, Pomper MG. Initial Evaluation of [18F]DCFPyL for Prostate-Specific Membrane Antigen (PSMA)-Targeted PET Imaging of Prostate Cancer. Molecular Imaging and Biology. 2015; 17:565–574. [PubMed: 25896814]
31. Lutje S, Heskamp S, Cornelissen AS, Poeppel TD, van den Broek SAMW, Rosenbaum-Krumme S, Bockisch A, Gotthardt M, Rijpkema M, Boerman OC. PSMA Ligands for Radionuclide Imaging and Therapy of Prostate Cancer: Clinical Status. Theranostics. 2015; 5:1388–1401. [PubMed: 26681984]
32. Rowe SP, Gorin MA, Allaf ME, Pienta KJ, Tran PT, Pomper MG, Ross AE, Cho SY. PET imaging of prostate-specific membrane antigen in prostate cancer: current state of the art and future challenges. Prostate Cancer Prostatic Dis. 2016
33. Chen Y, Pullambhatla M, Minn I, Wang Y, Jin J, Bhujwalla Z, Mease R, Pomper M. A PSMA-Targeted Theranostic Agent for Prostate Cancer. Journal of Nuclear Medicine. 2015; 56(3):1212. [PubMed: 26135110]
34. Wang X, Tsui B, Ramamurthy G, Zhang P, Meyers J, Kenney ME, Kiechle J, Ponsky L, Basilion JP. Theranostic Agents for Photodynamic Therapy of Prostate Cancer by Targeting Prostate Specific Membrane Antigen. American Association for Cancer Research. 2016
35. Cheng Y, Prusoff WH. Relationship between the inhibition constate (K1) and the concentration of inhibitor which causes 50 percent inhibition (I50) of an enzymatic reaction. Biochem Pharmcol. 1973; 22:3099–3108.
36. Chen Y, Foss CA, Byun Y, Nimmagadda S, Pullambhatla M, Fox JJ, Castanares M, Lupold SE, Babich JW, Mease RC, Pomper MG. Radiohalogenated prostate-specific membrane antigen (PSMA)-based ureas as imaging agents for prostate cancer. Journal of medicinal chemistry. 2008; 51:7933–7943. [PubMed: 19053825]
37. Silver DA, Pellicer I, Fair WR, Heston WD, Cordon-Cardo C. Prostate-specific membrane antigen expression in normal and malignant human tissues. Clin Cancer Res. 1997; 3:81–85. [PubMed: 9815541]

Highlights

- **YC-9** was synthesized as a PSMA-targeted theranostic agent for photodynamic therapy.
- PSMA-specific tumor uptake of **YC-9** was observed with in vivo optical imaging.
- PSMA-specific in vitro cell kill was achieved through **YC-9** PDT.
- Tumor growth delay was achieved with **YC-9** PDT in a mouse model of prostate cancer.

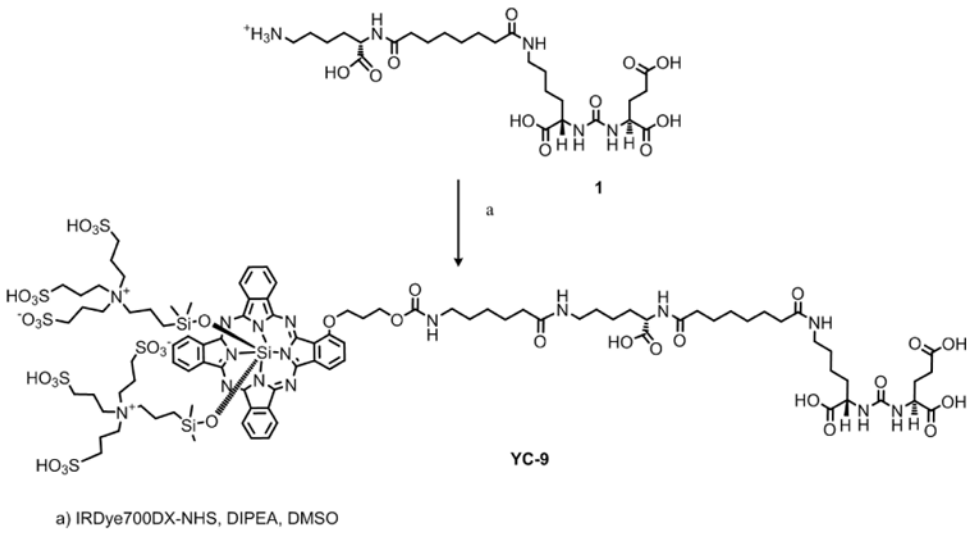

Figure 1. Synthesis of YC-9

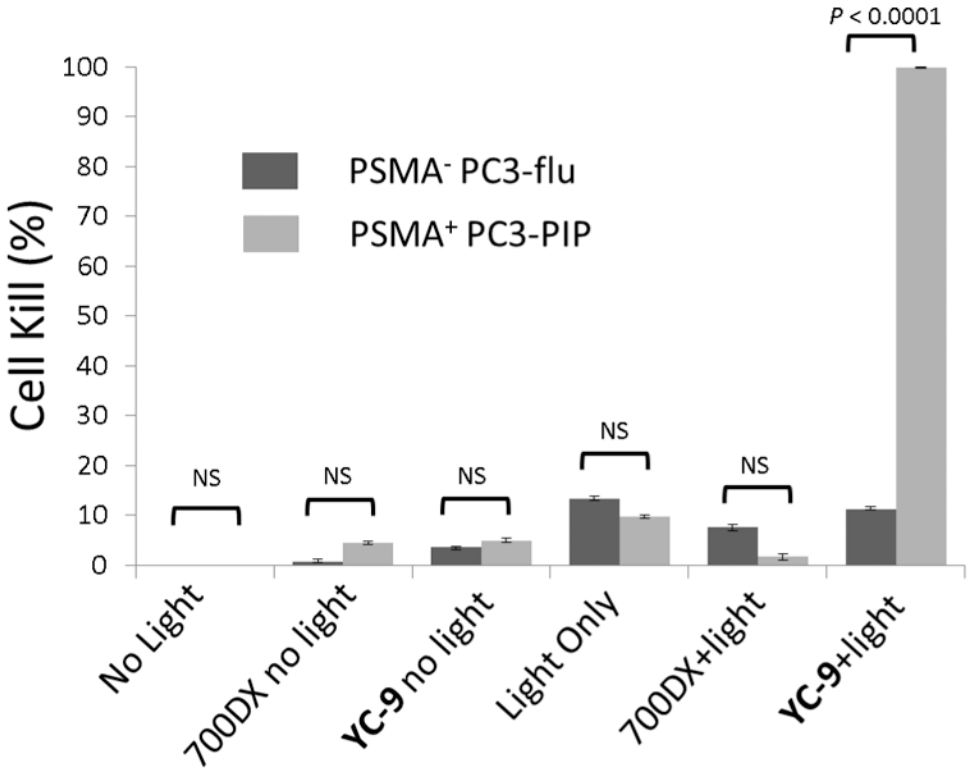

Figure 2.

YC-9 efficiently and specifically kills PSMA-expressing cells *in vitro*. PSMA$^+$ PC3-PIP and PSMA$^-$ PC3-flu cells were incubated with no dye, IRDye700DX (100 nM), and **YC-9** (100 nM) for 1 h at 37°C. After washing twice with media, cells were either irradiated with 2J/cm^z of 690 nm NIR light or were not irradiated. Cell kill was measured by XTT assay 24 hr post irradiation. Error bars represents standard deviation (n = 4). Student's *t*-test demonstrated a significant difference in cell kill only for the group treated with Light+**YC-9**, NS: not significant.

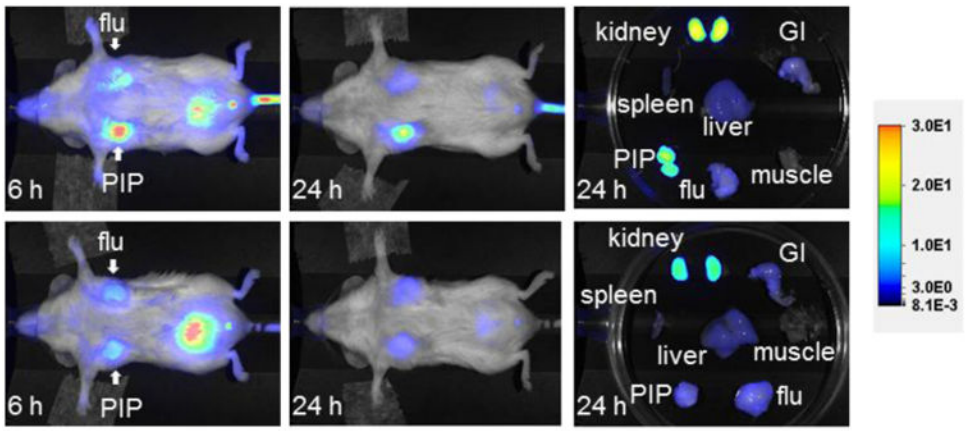

Figure 3.

Top row: Images after administration of 10 nmol of **YC-9** at 6 and 24 h post-injection, as well as images of the excised organs at 24 h post-injection. Bottom row: Image after administration of 10 nmol of **YC-9** and 1 mmol of DCIBzL, a high-affinity ligand forPSMA (blocker) at the same time points as above. Note lack of uptake in the mouse with DCIBzL, indicating binding specificity.

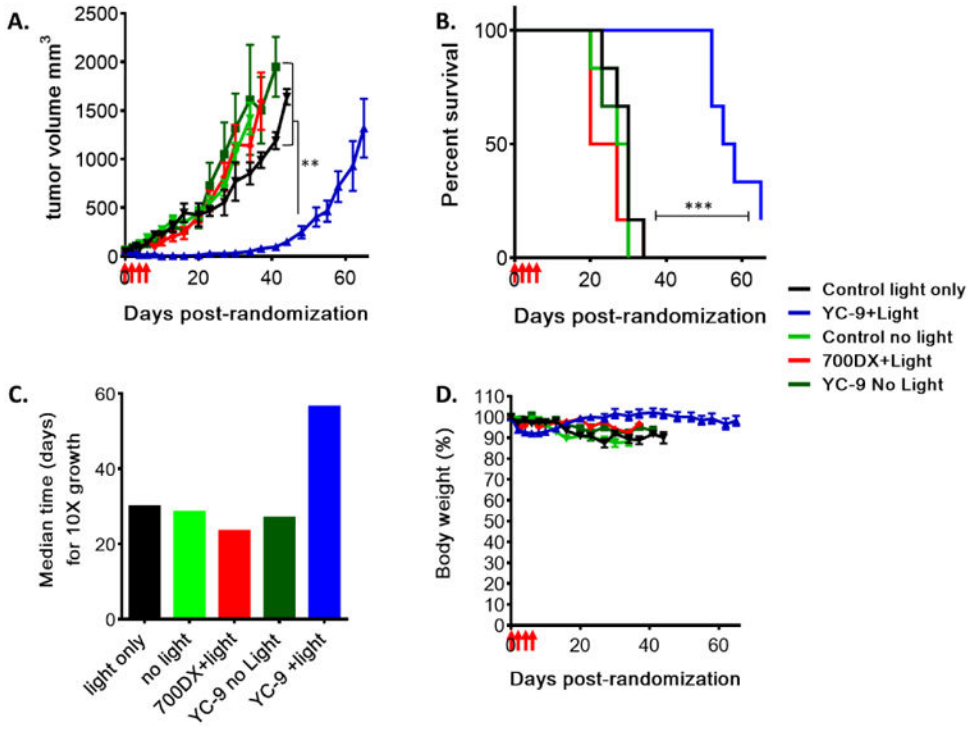

Figure 4. ***In vivo*** **PDT study with YC-9**

Mice with ~50 mm^3 $PSMA^+$ PC3-PIP tumors were randomized into five treatment groups (n=6) : 1) **YC-9** + light, 2) Light alone, 3) non-targeted IRDye700DX + light, 4) **YC-9** without light and 5) untreated control without light. Four doses of **YC-9** or non-targeted IRDye700DX (10 nmol each, in PBS) were injected intravenously, 48 h apart. Four hours after injection, the tumor surface of each mouse was superficially irradiated with an LED light source (wavelength: 690 ± 20 nm, total fluence: 100 J/cm^2), while **YC-9** without light and the untreated control group received no light treatment. **(A)** Tumor growth curves in different treatment groups. Statistical significance was calculated using one-way ANOVA. **(B)** Kaplan-Meier plot showing delayed tumor growth in the **YC-9**+ light treatment group. Tumor growth progression was plotted as number of days taken for a tumor to reach a ten-fold increase of the initial tumor volume. **(C)** Median time to reach a ten-fold increase of the initial tumor size in different treatment groups, derived from the Kaplan-Meier plot. **(D)** Mouse body weights are shown as a percentage of initial pretreatment weights. Four red arrows on the X-axis indicate the start of PDT treatment (**, $P < 0.01$; ***, $P < 0.001$).

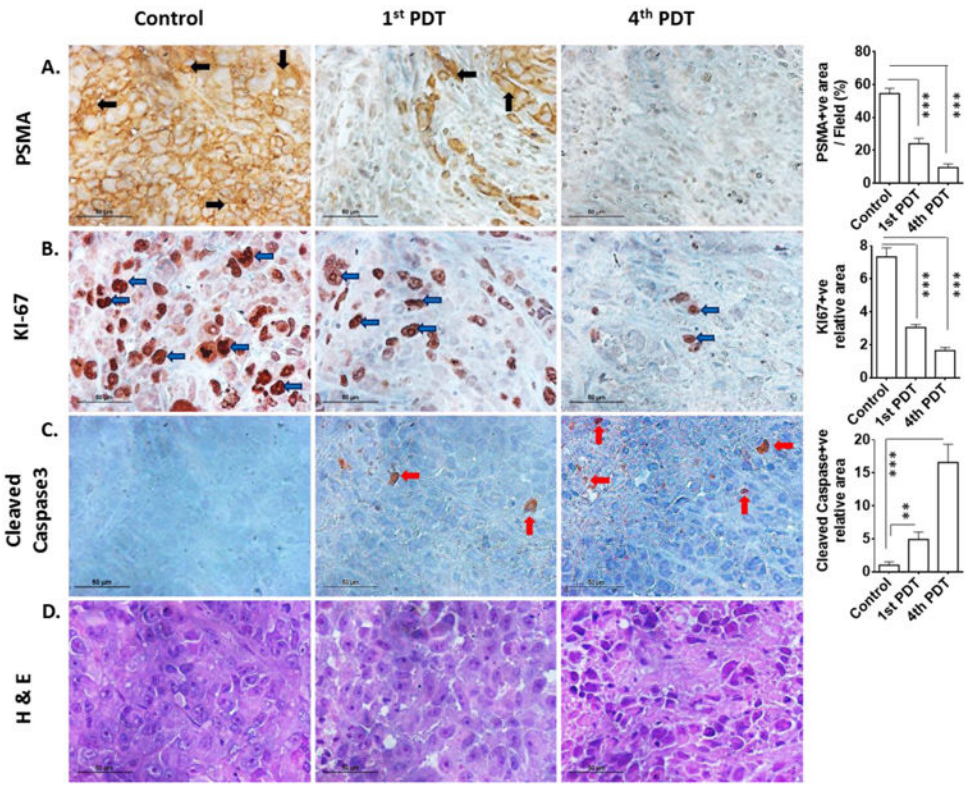

Figure 5. Histological assessment of tumor sections after PDT treatment

(A) PSMA$^+$ PC3-PIP untreated control tumor and one or four doses of **YC-9** PDT-treated tumor sections were stained with anti-PSMA, **(B)** anti-Ki-67, **(C)** anti-cleaved caspase-3 and **(D)** H&E. All images were acquired at 40× magnification. Scale bars represent 50 μm for all panels. The graphs at the right most column describe quantification of the corresponding immunohistochemical staining. PDT-treated PSMA$^+$ PC3-PIP tumor showed reduced PSMA expression, increased cell death (H&E and anti-caspase-3) and lower cellular proliferation (Ki-67) compared to control tumor (**, $P < 0.01$; ***, $P < 0.001$).

Table 1

***In vivo* photodynamic therapy treatment groups**

Group	1	2	3	4	5
Photosensitizer (iv injection)	**YC-9** (10 nmol)	-	IRDye700DX (10 nmol)	**YC-9** (10 nmol)	-
Light Treatment	100 J/cm^2 at 4 h pi	100 J/cm^2 at 4 h pi	100 J/cm^2 at 4 h pi	-	-